Spectrochimica Acta Part A 72 (2009) 36–40

Contents lists available at ScienceDirect

Spectrochimica Acta Part A: Molecular and Biomolecular Spectroscopy

journal homepage: www.elsevier.com/locate/saa

Solvent induced shifts of electronic spectra IV. Computational study on PRODAN fluorescence and implications to the excited state structure

Snezhana M. Bakalova*, Jose Kaneti

Institute of Organic Chemistry with Centre of Phytochemistry, Bulgarian Academy of Sciences, Acad. G. Bonchev Str., Block 9, 1113 Sofia, Bulgaria

ARTICLE INFO

Article history:
Received 13 February 2008
Received in revised form 9 July 2008
Accepted 15 July 2008

Keywords:
PRODAN fluorescence
Solvent effects
Computational modeling
CISD AM1
TD DFT
PICT

ABSTRACT

Vertical S_1–S_0 electronic transitions of the highly solvent-sensitive fluorescence label 2-propionyl-6-dimethylamino naphthalene (PRODAN) are modeled by semiempirical CISD AM1 and TD DFT calculations in a large number of solvents of different polarity and hydrogen donating ability. Calculations correctly reproduce the observed solvent induced shifts of the emission maxima. The fluorescence Frank-Condon transition energies in solvent can be predicted quantitatively at the AM1 SM5.42 OPEN(2,2) C.I. = 5 CISD level. For the planar PRODAN emitting state at the latter level we obtain a regression with practically unit slope and zero intercept for aprotic solvents. The respective relationship for the O-twisted S_1 state has a slope of 0.59 and intercept of 9100 cm^{-1}. These results support the concept that no geometry twist in the S_1 state of PRODAN is necessary to explain the observed solvent effects on fluorescence.

1. Introduction

Recently we have reported a CISD [1] AM1 [2] computational model for prediction of the energies of the electronic (absorption and fluorescence) transitions of organic molecules, as well as their solvent dependence [3]. The model is based on a part of the Jablonsky diagram [4] and includes explicit geometry optimization of the S_0 and S_1 electronic states in different solvents. Our computational cycle consists of the following steps:

1. CISD calculation of the equilibrium geometry of the S_0 electronic state of the solute, with full geometry relaxation.
2. Single point CISD calculation of the S_1 energy at the S_0 geometry to compute the corresponding vertical $S_0 \rightarrow S_1$ absorption transition energy.
3. CISD calculation of the equilibrium geometry of the S_1 (or, possibly, T_1) electronic state of the solute, with full geometry relaxation.
4. Single point CISD calculation of the S_0 energy at the S_1 (or, possibly, the T_1) geometry to compute the energy of the corresponding vertical $S_1 \rightarrow S_0$ or $T_1 \rightarrow S_0$ emission transition.

On the basis of the reasonable success in accounting for the observed solvent effects on the electronic spectra of several classes of chromophores using the above "relaxation cycle" [3,5], we consider the outlined methodology a suitable approximation for systematic studies of structural changes in the lowest molecular excited states as well.

To account for the solvent effect we use the Conductor-like Solvent Model, COSMO [6–8] at the AM1 and PM3 semiempirical levels of theory. However, COSMO is treating explicitly only the electrostatic components of solvent–solute interactions and could potentially lead to fallacious predictions of electronic absorption and emission Frank-Condon transition energies. Therefore we now check out also the performance of an arguably better treatment of continuum solvent–solute interactions as offered by the charge model of Cramer and Truhlar [9,10] in its SM5.42 form [11,12] still at the level of semiempirical MO theory. To verify the computational results, we use the thorough experimental data on the photophysical characteristics of 2-propionyl-6-dimethylamino naphthalene, PRODAN [13–15]. PRODAN is one of the best known highly solvent-sensitive fluorophores and is used extensively as a fluorescent probe for micropolarity in various chemical and biological systems.

Another issue we address on the basis of our computational results is the nature of the lowest excited singlet (fluorescent) state, S_1, of PRODAN. While the number of reports on PRODAN applications constantly increases, the nature of its S_1 state is still under discussion. Planar intramolecular charge transfer (PICT) S_1 state, as well as twisted intramolecular charge transfer S_1 state (TICT model) arising from twisting of either the $-N(CH_3)_2$ (N-TICT) or the $C(=O)-CH_2CH_3$ group (O-TICT) out of the plane of the naphthalene ring have been suggested for explanation of the emission properties

* Corresponding author. Tel.: +359 2 9606126; fax: +359 2 8700225.
E-mail address: bakalova@orgchm.bas.bg (S.M. Bakalova).

1386-1425/$ – see front matter © 2008 Elsevier B.V. All rights reserved.
doi:10.1016/j.saa.2008.07.020

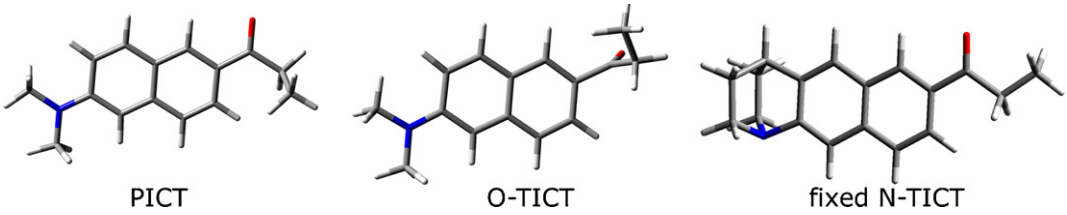

Fig. 1. Optimized geometries of PRODAN PICT and O-TICT conformers in acetonitrile in the S_1 state, AM1 with keywords C.I. = 5 OPEN(2,2) ROOT = 2, SM5.42. Blue is nitrogen, and red is oxygen. Also shown is a fixed model of the suggested N-TICT structure [19]. (For interpretation of the references to color in this figure legend, the reader is referred to the web version of the article.)

of PRODAN [14,16–18]. In our opinion, recent experimental studies on model naphthalene derivatives in which the dimethylamino group is constrained to be either coplanar [14] or perpendicular [19] (fixed N-TICT, Fig. 1) with the naphthalene ring, show unambiguously that no N-TICT contributes to PRODAN emission. Thus, the planar (PICT) and twisted perpendicular carbonyl (O-TICT) conformations of PRODAN S_1 state shown in Fig. 1 still remain under discussion.

2. Computational details

General-purpose semiempirical MO methods such as MINDO/3, MNDO, PM3 and AM1 are primarily concerned with the prediction of ground state molecular properties at equilibrium geometries. This is where the vast majority of data exist and where the methods were parametrized. However, there are several classes of molecular properties where this first-level parametrization is not applicable. Perhaps the most obvious of them is the description of excited states for the prediction of UV/Vis spectra. The need for efficient semiempirical methods capable of calculating these quantities has long been recognized, especially in cases of larger molecules. Dedicated methods parametrized specifically for this application have been proposed and implemented [20,21]. The latter approaches are based on a post-SCF configuration interaction (C.I.) variational formalism restricted to single excitations (SCF-CIS). More sophisticated methods can indeed take into account double and higher electron excitations.

Semiempirical AM1 MO calculations in the present paper are carried out with the MOPAC 2007 [8] and the AMSOL (version 7.1) [11] program packages. Gradient geometry optimizations are done initially for the closed shell ground state structure S_0, as in earlier MO studies of electronic absorption spectra. However, we further optimize the excited S_1 geometry including configuration interaction C.I. [22] using the microstate formalism [1] with a limited number of single and double excitations, namely two electrons in two orbitals, with a total of 4–7 active orbitals. All optimizations are carried with the EF procedure of Baker [23,24]. Gradient norm less than 0.05 kcal mol^{-1} A^{-1} is achieved for all values of ε between 2 and 80 for the entire range of solvents used in the experiment [14,15] in the COSMO optimizations. The same degree of optimization is not always possible for the excited S_1 state with AMSOL. In such cases the procedure has been persistently repeated with corresponding structures to reduce the gradient norm to less than 1.0 kcal mol^{-1} A^{-1}. The positions of the fluorescence maxima are calculated as vertical singlet transition energies $S_1 \rightarrow S_0$ at the optimized geometry of the S_1 species. We note that the final reduction of gradient norm from 1.0 to below 0.05 kcal mol^{-1} A^{-1} changes the $S_1 \rightarrow S_0$ transition energy by only ca. 5 cm^{-1}.

The solvent effect on electron transition energies of interest is accounted for by two implicit continuum solvent models. The more simple of these, the Conductor-like Screening Model (COSMO) has been developed by Klamt and Schüürmann [6,7] and assumes that the surrounding medium is well modeled as a conductor, which simplifies the electrostatics computations. This is approximated by calculation of apparent surface charges on the solute cavity surface. If necessary, corrections can be made a posteriori for dielectric behavior.

The more sophisticated SMx models, $x = 1–8$ [25,26] combine electrostatics with additional terms for first-solvation-shell effects, as well as for bulk solvent properties. Among these are the surface tension, the index of refraction, etc. The solvent response to solute presence is better accounted for via distributed partial charges within the solute, termed charge model 1–4 class I–IV charges [25,26]. The SM5.42 version, used in this paper, includes CM2 class IV charges. The greater flexibility of the latter partial charge models has the expected consequence of better representation of observed solvent effects.

Single point time dependent DFT calculations at the optimized semiempirical geometries are performed using GAUSSIAN03 [27]. Solvent effects are accounted for by the CPCM [6,28] (similar to COSMO) and the PCM [29] formalisms.

3. Results and discussion

AM1 results show that both the PICT and O-TICT S_1 structures are minima on the S_1 potential energy surface and possibly exist in solution at equilibrium. The experimental fluorescence data and the computed vertical S_1–S_0 electronic transition energies of PRODAN in various solvents are compared in Table 1. Separate linear regressions, for aprotic and protic solvents, respectively, between the experimental and calculated energies of the emission maxima for each of the two conformers (PICT and O-TICT) have drastically different slopes and much higher correlation coefficients than the respective common relationships including all solvents (see Table 2 and Fig. 2). This observation is in agreement with the deduction derived from experimental data, that the nature of the emitting state in aprotic and protic solvents is different, presumably due to hydrogen bonding of PRODAN in the S_1 intramolecular charge transfer (ICT) electronic state with protic solvents [15,16,31,32], suggested also for other molecules with ICT excited electronic states [3,32]. It also lends additional support to the reliability of the computed solvent shifts of PRODAN fluorescence maximum.

Regression analyses of the theoretical AM1 predictions for PRODAN (PICT S_1 state) versus experimental data in aprotic solvents (see Table 2) indicate that (i) the charge model SM5.42 is better than COSMO; and (ii) the C.I. = 5 configuration space of CISD is better than C.I. = 6 for SM5.42. Particularly gratifying is the correlation of calculated SM5.42 C.I. = 5 vs. experimental emission maxima for aprotic solvents (Fig. 2) with practically unit slope and negligible intercept.

More detailed inspection of the regression between experimental fluorescence maxima of PRODAN in aprotic solvents and calculated CISD AM1 vertical S_1–S_0 energies for its PICT conformer (Fig. 2) shows three distinct outliers – the two aromatic solvents benzene and toluene, as well as formamide. The former possibly indicate some additional aromatic solvent–aromatic solute inter-

Table 1
Fluorescence maxima (ν_F^{exp} (cm^{-1})) and computed energies of the vertical S_1–S_0 transitions (ν_F^{calc} (cm^{-1})) of the PICT and O-TICT conformers of PRODAN in a series of solvents.

Solvent	$E_T(30)$[a]	ν_F^{exp}	PICT				O-TICT	
			ν_F^{calc} SM5.42, C.I. = 5	ν_F^{calc} SM5.42, C.I. = 6	ν_F^{calc} COSMO, C.I. = 5	ν_F^{calc} COSMO, C.I. = 6	ν_F^{calc} SM5.42, C.I. = 5	ν_F^{calc} COSMO, C.I. = 5
n-Hexane	30.9	25,630[b]	25,336	24,741	25,561	24,942	24,311	24,544
Heptane	31.1	25,650[b]	25,306	24,727	25,543	24,929	24,290	24,528
Cyclohexane	31.2	25,650[b]	25,215	24,669	25,477	24,882	24,228	24,473
Toluene	33.9	24,040[b]	24,946	24,437	25,267	24,728	24,043	24,304
Benzene	34.5	23,990[b]	25,017	24,509	24,343	24,577	24,084	24,350
THF	37.4	23,300[b]	23,029	22,361	23,691	23,092	22,860	23,192
Ethylacetate	38.1	23,256[a]	23,346	22,734	23,971	23,408	23,055	23,376
Acetone	42.2	22,520[b]	21,912	21,107	22,698	21,952	22,254	22,570
DMF	43.8	22,090[b]	21,560	20,692	22,367	21,565	22,061	22,368
DMSO	45.0	21,552[a]	21,459	20,566	22,275	21,457	22,011	22,314
Acetonitrile	46.0	21,900[b]	21,582	20,711	22,385	21,587	22,065	22,381
Formamide	56.6	20,100[b]	21,231	21,544	22,060	21,208	21,895	22,189
2-Propanol	48.6	21,070[b]	21,974	21,168	22,743	22,004	22,285	22,598
Ethanol	51.9	20,350[b]	21,801	20,933	22,574	21,807	22,181	22,494
Methanol	55.5	19,920[b]	21,630	20,785	22,379	21,636	22,096	22,406
1,2-Ethanediol	56.3	19,760[b]	21,528	20,668	22,333	21,526	22,045	22,349
1-Butanol	–	20,730[b]	22,052	21,262	22,824	22,098	22,329	22,647
Water	63.1	19,030[b]	21,323	20,431	22,124	21,286	21,923	22,227

$E_T(30)$ is an empirical solvent polarity parameter (in kcal mol^{-1}) [30]. Used program keywords are MECI OPEN(2,2) SINGLET ROOT = 2.
[a] Ref. [14].
[b] Ref. [15].

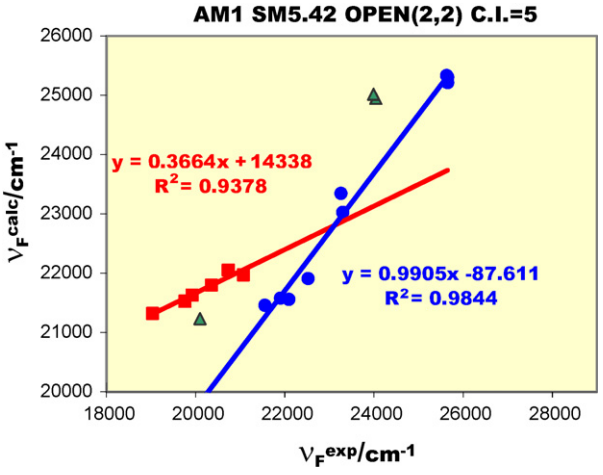

Fig. 2. Relationships between experimental and computed energies of fluorescence maxima of the planar (PICT) conformer of PRODAN: aprotic solvents in blue circles and protic solvents in red squares. Green triangles at calculated wavenumbers ca. 25,000 cm^{-1} correspond to benzene and toluene. The green triangle at calculated wavenumber ca. 21,000 cm^{-1} corresponds to formamide. See text for discussion. (For interpretation of the references to color in this figure legend, the reader is referred to the web version of the article.)

actions, e.g. PRODAN–benzene complexes/exciplexes. Formamide, on the other hand, has conceivable characteristics of both protic and aprotic solvent and in the case of relatively basic solute PRODAN, resembles a protic rather than aprotic solvent.

The almost perfect relationship of AM1 SM5.42 calculated emission energies of PRODAN in its completely optimized PICT S_1 state vs. experimental fluorescence maxima in aprotic solvents allows a revisit of the intensely disputed geometry of PRODAN emitting state. The AM1 predicted Frank-Condon emission energies of the O-TICT structures (see Tables 1 and 2) in aprotic solvents correlate with experimental data reasonably well. However, the predicted wavelengths are systematically blue shifted relative to experiment, so the slopes of the O-TICT relationships are significantly different from 1 and the corresponding intercepts are huge, in contrast to those obtained with PICT structures for aprotic solvents. This casts certain doubt on the relevance of O-TICT to the observed PRODAN emission spectra in aprotic solvents.

To additionally check the latter result, we also calculate solvent shifts in planar and perpendicular conformations of PRODAN by means of single point time dependent density functional, TD PBE1PBE/6-31 + G** [33,34], solvent calculations [35] at the optimized semiempirical CISD AM1 SM5.42 C.I. = 5 S_1 state geometries in cyclohexane and acetonitrile (see Table 3). Notably, calculated full DFT energies of planar PRODAN structures are lower than those of perpendicular O-TICT ones by some 30–36 kJ mol^{-1}, meaning that the latter cannot be considered abundant in the S_1 state.

Table 2
Regression analyses of experimental fluorescence maximum energies vs. AM1 computational results for planar (PICT) and perpendicular (O-TICT) PRODAN with varying solvent models and CISD configuration space for aprotic and protic solvents.

Conformer	PICT				O-TICT	
Method	SM5.42, C.I. = 5	SM5.42, C.I. = 6	COSMO, C.I. = 5	COSMO, C.I. = 6	SM5.42, C.I. = 5	COSMO, C.I. = 5
Aprotic solvents						
R^2	0.984	0.981	0.981	0.973	0.987	0.986
Slope	0.991	1.067	0.838	0.885	0.591	0.571
Intercept	88	2604	4085	2282	9128	9887
Protic solvents						
R^2	0.938	0.934	0.933	0.936	0.939	0.935
Slope	0.366	0.412	0.351	0.402	0.202	0.208
Intercept	14340	12580	15435	13620	18076	18258

Table 3
TD PBE1PBE/6-31 + G(d,p) calculated S_1 and vertical S_1–S_0 energies of PICT and O-TICT PRODAN conformers at the respective optimized S_1 AM1 SM5.42 geometries in cyclohexane and acetonitrile.

Solvent	TD PBE1PBE/6-31 + G(d,p)//CISD AM1					
	Gas phase		CPCM		PCM	
	Full energy (au)	S_1–S_0 (cm^{-1})	Full energy (au)	S_1–S_0 (cm^{-1})	Full energy (au)	S_1–S_0 (cm^{-1})
PICT						
Cyclohexane	−711.01534	26,939	−711.02323	25,749	−711.02137	25,878
Acetonitrile	−711.01476	27,028	−711.03242	24,924	−711.03208	25,012
O-TICT						
Cyclohexane	−711.00391	27,884	−711.01205	27,303	−711.00993	27,375
Acetonitrile	−711.00093	27,673	−711.01881	26,721	−711.01841	26,778

Each entry is represented by data in the gas phase, cyclohexane and acetonitrile. Solvent effects are calculated by the continuum CPCM (COSMO) and PCM models.

This conclusion is in agreement with the experimentally observed single-exponential fluorescence decay in both nonpolar and polar aprotic solvents [16].

The gas phase TD PBE1PBE/6-31 + G(d,p) calculations at the corresponding AM1 solvent geometries show small geometry effect (cyclohexane to acetonitrile) on the S_1–S_0 transition: hypsochromic (90 cm^{-1}) for the planar (PICT) conformer and bathochromic (210 cm^{-1}) for the perpendicular (O-TICT) conformer, respectively. Solvent TD PBE1PBE/6-31 + G(d,p) calculations at the same geometries more than offset the above geometry effect. As seen from Table 3, both for the planar (PICT) and the significantly less stable perpendicular (O-TICT) PRODAN S_1 conformer, solvent effects on the S_1–S_0 vertical transition energy generally follow the experimentally observed trend of bathochromic displacement upon increase of solvent polarity, but predicted solvent shifts are much lower than the experimentally determined ones: both CPCM and PCM predict a red shift of ca. 850 cm^{-1} for the PICT conformer and ca. 600 cm^{-1} for the O-TICT conformer from cyclohexane to acetonitrile. It should be noted that the TD DFT vertical S_1–S_0 energies calculated by both CPCM and PCM for PICT PRODAN in cyclohexane are very close to the experimentally determined value while predicted O-TICT emission Frank-Condon energies are ca. 1800 cm^{-1} higher.

The difference between the energies of the emission maxima of PRODAN in acetonitrile and methanol, which have similar polarity (ca. 2000 cm^{-1}) can serve as a rough estimate of the stabilization energy of the S_1 state due to hydrogen bonding between the solute and protic solvents [3]. Correcting the AM1 SM5.42 C.I. = 5 calculated S_1–S_0 vertical emission energies for planar PRODAN in protic solvents with the additional stabilization energy, estimated above, we obtain a common relationship for all solvents between experimental and calculated Frank-Condon fluorescence energies with slope 0.988 and intercept −88 cm^{-1} (R^2 = 0.978). This result indicates that the PICT structure is the prevailing one in protic solvents as well.

4. Conclusions

Fluorescence maxima shifts depend on both geometry and electronic structure changes, amplified to a significant extent by the solvent, and are correctly modeled by present calculations. The experimental range of bathochromic shift of PRODAN emission for aprotic solvents (from *n*-hexane to dimethylsulfoxide) is ~4100 cm^{-1}. The PICT model at the AM1 CISD level (SM5.42 C.I. = 5) predicts a range of ca. 3900 cm^{-1}, and the respective regression has a practically unit slope and zero intercept. In contrast, the predicted range for the O-TICT model amounts only to ~2300 cm^{-1} with the respective regression having a slope of 0.59 and intercept 9100 cm^{-1}. Our results thus support the assumption that no geometry change in the S_1 state of PRODAN is necessary to explain the observed spectroscopic phenomena. Twisting of the carbonyl group out of the plane of the naphthalene ring should result in hypsochromic shift of the fluorescence maxima in disagreement with experiment.

From the viewpoint of computational methodology, both semiempirical and TD DFT calculations correctly reproduce the observed trends in solvent spectroscopic shifts. TD DFT results however can only be compared to fluorescence experiment in the qualitative sense, while the predictive capability of AM1 SM5.42 CISD calculations is quantitative.

Acknowledgment

We thank J.J.P. Stewart for fruitful discussions and encouragement.

References

[1] D.R. Armstrong, R. Fortune, P.G. Perkins, J.J.P. Stewart, J. Chem. Soc. Faraday Trans. 2 68 (1972) 1839.
[2] M.J.S. Dewar, E.G. Zoebisch, E.F. Healy, J.J.P. Stewart, J. Am. Chem. Soc. 107 (1985) 3902.
[3] S. Bakalova, J. Kaneti, Spectrochim. Acta A 56 (2000) 1443 (part III in this series).
[4] J.R. Lakowicz, Principles of Fluorescence Spectroscopy, 2nd ed., Kluwer Academic/Plenum, New York, 1999.
[5] S.M. Bakalova, A. Gil Santos, I. Timcheva, J. Kaneti, I.L. Philipova, G.M. Dobrikov, V.D. Dimitrov, J. Mol. Struct. (Theochem.) 710 (2004) 229.
[6] A. Klamt, G. Schüürmann, J. Chem. Soc. Perkin Trans. 2 (1993) 799.
[7] A. Klamt, J. Phys. Chem. 100 (1996) 3349.
[8] J.J.P. Stewart, J. Mol. Mod. 13 (2007) 1173;
J.J.P. Stewart, Stewart Computational Chemistry, Colorado Springs, CO, USA, 2007, http://OpenMOPAC.net.
[9] C.J. Cramer, D.G. Truhlar, J. Am. Chem. Soc. 113 (1991) 8305, 9901(E).
[10] J. Li, J. Xing, C.J. Cramer, D.G. Truhlar, J. Chem. Phys. 111 (1999) 885.
[11] G.D. Hawkins, D.J. Giesen, G.C. Lynch, C.C. Chambers, I. Rossi, J.W. Storer, J. Li, T. Zhu, J.D. Thompson, P. Winget, B.J. Lynch, D. Rinaldi, D.A. Liotard, C.J. Cramer, D.G. Truhlar, Department of Chemistry and Supercomputer Institute, Univ. Minnesota, Minneapolis, Minnesota 55455-0431, USA; http://comp.chem.umn.edu/amsol/, 2004.
[12] J. Li, T. Zhu, G.D. Hawkins, P. Winget, D.A. Liotard, C.J. Cramer, D.G. Truhlar, Theor. Chem. Acc. 103 (1999) 9.
[13] G. Weber, F.J. Farris, Biochemistry 18 (1979) 3075.
[14] B.C. Lobo, C.J. Abelt, J. Phys. Chem. A 107 (2003) 10938.
[15] F. Moyano, M.A. Biasutti, J.J. Silber, N.M. Correa, J. Phys. Chem. B 110 (2006) 11838.
[16] A. Samanta, R.W. Fessenden, J. Phys. Chem. A 104 (2000) 8972.
[17] A.B.J. Parusel, W. Nowak, S. Grimme, G. Köhler, J. Phys. Chem. A 102 (1998) 7149.
[18] A. Parusel, J. Chem. Soc. Faraday Trans. 94 (1998) 2923.
[19] B.N. Davis, C.J. Abelt, J. Phys. Chem. A 109 (2005) 1295.
[20] J. Del Bene, H.H. Jaffe, J. Chem. Phys. 48 (1968) 1807;
J. Del Bene, H.H. Jaffe, J. Chem. Phys. 48 (1968) 4050;
J. Del Bene, H.H. Jaffe, J. Chem. Phys. 49 (1968) 122;
J. Del Bene, H.H. Jaffe, J. Chem. Phys. 50 (1969) 1126.
[21] J. Ridley, M.C. Zerner, Theor. Chim. Acta (Berl.) 32 (1973) 111.
[22] M.J.S. Dewar, D.A. Liotard, J. Mol. Struct. (Theochem.) 206 (1990) 123.
[23] J. Baker, J. Comput. Chem. 7 (1986) 385.
[24] F. Jensen, J. Chem. Phys. 102 (1995) 6706.
[25] C.J. Cramer, D.G. Truhlar, Chem. Rev. 99 (1999) 2161.
[26] C.J. Cramer, D.G. Truhlar, Acc. Chem. Res. 41 (2008) 760.

[27] M.J. Frisch, G.W. Trucks, H.B. Schlegel, G.E. Scuseria, M.A. Robb, J.R. Cheeseman, J.A. Montgomery Jr., T. Vreven, K.N. Kudin, J.C. Burant, J.M. Millam, S.S. Iyengar, J. Tomasi, V. Barone, B. Mennucci, M. Cossi, G. Scalmani, N. Rega, G.A. Petersson, H. Nakatsuji, M. Hada, M. Ehara, K. Toyota, R. Fukuda, J. Hasegawa, M. Ishida, T. Nakajima, Y. Honda, O. Kitao, H. Nakai, M. Klene, X. Li, J.E. Knox, H.P. Hratchian, J.B. Cross, C. Adamo, J. Jaramillo, R. Gomperts, R.E. Stratmann, O. Yazyev, A.J. Austin, R. Cammi, C. Pomelli, J.W. Ochterski, P.Y. Ayala, K. Morokuma, G.A. Voth, P. Salvador, J.J. Dannenberg, V.G. Zakrzewski, S. Dapprich, A.D. Daniels, M.C. Strain, O. Farkas, D.K. Malick, A.D. Rabuck, K. Raghavachari, J.B. Foresman, J.V. Ortiz, Q. Cui, A.G. Baboul, S. Clifford, J. Cioslowski, B.B. Stefanov, G. Liu, A. Liashenko, P. Piskorz, I. Komaromi, R.L. Martin, D.J. Fox, T. Keith, M.A. Al-Laham, C.Y. Peng, A. Nanayakkara, M. Challacombe, P.M.W. Gill, B. Johnson, W. Chen, M.W. Wong, C. Gonzalez, J.A. Pople, Gaussian 03, Revision C.02, Gaussian, Inc., Wallingford, CT, 2004.
[28] A. Klamt, V. Jonas, T. Buerger, J.C.W. Lohrenz, J. Phys. Chem. A 102 (1998) 5074.
[29] J. Tomasi, M. Persico, Chem. Rev. 94 (1994) 2027.
[30] C. Reichardt, Chem. Rev. 94 (1994) 2319.
[31] W.P. Zurawsky, S.F. Scarlata, J. Phys. Chem. 96 (1992) 6012.
[32] C.F. Chapman, R.S. Fee, M. Maroncelli, J. Phys. Chem. 99 (1995) 4811.
[33] R. Bauernschmitt, R. Ahlrichs, Chem. Phys. Lett. 256 (1996) 454.
[34] J.P. Perdew, K. Burke, M. Ernzerhof, Phys. Rev. Lett. 78 (1997) 1396.
[35] F. Eckert, A. Klamt, AIChE J. 48 (2002) 369.